ELSEVIER

Journal of Chromatography B, 736 (1999) 237–245

JOURNAL OF CHROMATOGRAPHY B

www.elsevier.com/locate/chromb

3-Hydroxyanthranilic acid-derived compounds formed through electrochemical oxidation

Hideo Iwahashi

Department of Chemistry, Wakayama Medical College, 811-1 Kimiidera, Wakayama 641-0012, Japan

Received 6 April 1999; received in revised form 5 October 1999; accepted 7 October 1999

Abstract

3-Hydroxyanthranilic acid (3-HAA)-derived oxidation products were analyzed using high-performance liquid chromatography with an electrochemical reactor and diode array detection and high-performance liquid chromatography with an electrochemical reactor and UV detection coupled with mass spectrometry. In addition to 3-HAA dimers such as cinnabarinic acid (CA), 6-amino-3-[(2-carboxy-6-hydroxyphenyl)amino]-2,5-dioxo-1,3-cyclohexadiene-1-carboxylic acid and 4,7-diamino-8-hydroxy-6H-dibenzo[*a*,*d*]pyran-6-one-3-carboxylic acid, a 3-HAA trimer and a 3-HAA tetramer were also detected and identified based on their electrospray ionization mass spectra and their UV–visible spectra. These five oxidation products were also detected on the elution profiles of high-performance liquid chromatography–diode array detection analyses for the reaction mixtures of the auto-oxidation of 3-HAA, of 3-HAA with potassium ferricyanide, of 3-HAA with horseradish peroxidase and hydrogen peroxide, and of 3-HAA with superoxide dismutase (SOD). 4,7-Diamino-8-hydroxy-6H-dibenzo[*a*,*d*]pyran-6-one-3-carboxylic acid was predominant in the auto-oxidation, in the reaction of 3-HAA with horseradish peroxidase and hydrogen peroxide, and in the electrochemical oxidation of 3-HAA at an applied potential of 0.0 V. On the other hand, CA, the 3-HAA trimer and the 3-HAA tetramer were predominant in the reaction of 3-HAA with $K_3[Fe(CN)_6]$ and in the electrochemical oxidation of 3-HAA at an applied potential of 1.0 V.

Keywords: 3-Hydroxyanthranilic acid; Cinnabarinic acid

1. Introduction

3-Hydroxyanthranilic acid (3-HAA) is an intermediate formed during oxidative tryptophan metabolism along the kynurenine pathway.

Recently, 3-HAA and 3-hydroxykynurenine have been reported to be antioxidants [1]. Christen et al. reported that interferon-γ inhibits human monocyte/macrophage-facilitated low density lipoprotein lipid peroxidation via induction of cellular tryptophan degradation and production and release of 3-HAA [2]. Furthermore, Thomas et al. reported that 3-HAA directly reduces α-tocopherol radical in UV-exposed micellar dispersions of α-tocopherol or in low density lipoprotein incubated with soybean 15-lipoxygenase [3]. In the above processes, 3-HAA works as co-antioxidant for α-tocopherol.

On the other hand, both 3-HAA and cinnabarinic acid (CA) are known carcinogens that have been linked to bladder and breast carcinomas [4–6]. Indeed, it has been shown that experimental cancer of the bladder can be induced by 3-HAA and 3-hydroxykynurenine [5]. In addition, a high incident of bladder tumors are demonstrated in rats fed with

0378-4347/99/$ – see front matter
PII: S0378-4347(99)00463-6

DL-tryptophan and 2-acetamidofluorene, whereas no bladder tumors are present in those animals fed with only supplemental 2-acetamidofluorene [7].

Since the oxidation of 3-HAA is supposed to be related to these carcinogenic and antioxidative activities, it is important to clarify the details of the oxidation of 3-HAA. Oxidation of 3-HAA has been investigated under various conditions. 3-HAA may undergo auto-oxidation with the production of H_2O_2 [8], superoxide radicals [8] and, in the presence of trace amounts of iron, hydroxyl radicals [9]. Conversion of 3-HAA to CA proceeds non-enzymatically through the reactions with Mn^{2+} ion and catalase [8,10], and with the thermolabile radical initiator 2,2′-azobis-2-amidinopropane under aerobic conditions [11]. Oxidation of 3-HAA is also mediated enzymatically [11–13]. Cinnabarinic acid formation is observed when 3-HAA is added to preformed compound I of horseradish peroxidase or catalytic amounts of either horseradish peroxidase, myeloperoxidase, or bovine liver catalase together with glucose/glucose oxidase [11]. The oxidative coupling of 3-HAA to form CA is also catalyzed by tyrosinase [12], laccase, blue copper oxidase and ceruloplasmin [13]. On the other hand, auto-oxidation of 3-HAA results in the formation of novel 3-HAA dimers such as 6-amino-3-[(2-carboxy-6-hydroxyphenyl)amino]-2, 5-dioxo-1, 3-cyclohexadiene -1-carboxylic acid and 4,7-diamino-8-hydroxy-6H-dibenzo[*a*,*d*]pyran-6-one-3-carboxylic acid [14,15].

Recently, several compounds have been detected and identified in the process of the oxidation of 3-hydroxykynurenine using high-performance liquid chromatography with an electrochemical reactor and UV detection coupled with mass spectrometry (HPLC–ED–UV–MS) and high-performance liquid chromatography with an electrochemical reactor and UV detection coupled with electron spin resonance spectrometry (HPLC–ED–UV–ESR) [16,17]. A guard cell of an electrochemical detector is placed between a HPLC injector and a HPLC column, and used as the electrochemical reactor in the HPLC–ED–UV–MS and the HPLC–ED–UV–ESR systems. In this paper, HPLC–ED–UV–MS and HPLC–ED–UV are employed to clarify the oxidation of 3-HAA. The 3-HAA-derived electrochemical oxidation products will be compared with those which form through auto-oxidation of 3-HAA, and reactions of 3-HAA with potassium ferricyanide, with horseradish peroxidase and hydrogen peroxide, and with superoxide dismutase (SOD).

2. Experimental

2.1. Materials

3-HAA was obtained from Tokyo Kasei Kogyo (Tokyo, Japan). Horseradish peroxidase was purchased from Oriental Yeast (Osaka, Japan). Bovine erythrocytes superoxide dismutase (SOD) (EC 1.15.1.1) and bovine liver catalase (EC 1.11.1.6.) were obtained from Sigma (St. Louis, MO, USA). Potassium ferricyanide was obtained from Wako (Osaka, Japan). Hydrogen peroxide was from Katayama (Osaka, Japan). All other chemicals used were of analytical grade.

2.2. HPLC–ED–UV

HPLC–ED–UV was recently applied to the elucidation of the redox reactions [16,17]. The HPLC–ED–UV system consisted of a Model 7125 Rheodyne injector with a 200-μl sample loop (Rheodyne, Cotati, CA, USA), a Model 655A-11 pump with a Model L-5000 LC controller (Hitachi, Ibaragi, Japan), a Model 5020 guard cell with a Model 5100A control module (ESA, Bedford, MA, USA), a column, and a Model SPD-M10AVP diode array detector with a Model CLASS-LC10 LC workstation (Shimadzu, Kyoto, Japan). The guard cell of the electrochemical detector was placed between the HPLC injector and the HPLC column. The Model SPD-M10AVP diode array detector was placed after the column.

The guard cell of the electrochemical detector was used as an electrochemical reactor in the HPLC–ED–UV system. The guard cell consisted of a reference electrode (Pd), a counter electrode, and a porous graphite electrode. Various oxidation potentials were set for the guard cell using the Model 5100A control module. The column (150 mm×4.6 mm I.D.) packed with TSKgel ODS-120T (5 μm particle size) (Tosoh, Tokyo, Japan) was used in the HPLC–ED–UV system. The pore size of the TSKgel ODS-120T was 120 Å. The column was kept at 25°C

throughout the analyses. The Model SPD-M10AVP diode array detector was operated from 200 nm to 700 nm. Signals from the diode array detector were monitored using the Model CLASS-LC10 LC workstation.

Two solvents were used in the HPLC–ED–UV analyses: (A) 50 m*M* acetic acid; (B) 50 m*M* acetic acid–methanol (10:90, v/v). A combination of isocratic and linear gradient was used for the HPLC–ED–UV experiments: 0–10 min, 100% A (isocratic) at flow-rate 0.1 ml/min; 10–11 min, 100% A (isocratic) at flow-rate 0.1 ml/min to 1.0 ml/min (linear increase); 11–40 min, 0% B to 100% B (linear gradient) at flow-rate 1.0 ml/min; 40–50 min, 100% B (isocratic) at flow-rate 1.0 ml/min.

Retention times of the peaks are mean±SD values for five determinations.

2.3. HPLC–ED–UV–MS

The HPLC–ED–UV–MS system consisted of a Model 7125 injector with a 200-μl sample loop (Rheodyne), a Model L-7100 pump (Hitachi), a Model 5020 guard cell with a Model 5100A control module (ESA), a column, a Model L-7400 UV detector (Hitachi), and a Model M-1200AP LC–MS system with an electrospray ionization (ESI) instrument (Hitachi). The guard cell of the electrochemical detector was placed between the HPLC injector and the HPLC column. The UV detector was placed after the column. The eluent from the UV detector was introduced into the LC–MS system.

The guard cell of the electrochemical detector was used as an electrochemical reactor in the HPLC–ED–UV–MS system. The oxidation potential of the guard cell was set at +0.5 V using the Model 5100A control module. The column (150 mm×4.6 mm I.D.) packed with TSKgel ODS-120T (5 μm particle size) (Tosoh) was used in the HPLC–ED–UV–MS system. The column was kept at 25°C throughout the analyses. The UV detector was operated at 380 nm. The operating conditions of the LC–MS system were: nebulizer, 180°C; aperture 1, 120°C; N_2 controller pressure, 1.9×10^5 Pa; drift voltage, 70 V; multiplier voltage, 1800 V; needle voltage, 3000 V; polarity, positive; resolution, 48.

Conditions of the mobile phase were as described for HPLC–ED–UV except for the LC–MS system. The mass spectra of peaks 2, 3, 4, 5 and 6 were obtained by introducing the eluent from the UV detector into the LC–MS system just before the respective peak was eluted. The flow-rate of the pump was kept at 50 μl/min while the eluent was introduced into the LC–MS system.

2.4. HPLC–UV

The HPLC–UV system was almost same as the HPLC–ED–UV system except for the ED part. A Model 5020 guard cell with a Model 5100A control module (ESA) was removed in the HPLC–UV system. Mobile phase conditions for HPLC–UV were as described for HPLC–ED–UV.

2.5. Samples for HPLC–ED–UV and HPLC–ED–UV–MS

3-HAA was dissolved in 50 m*M* sodium phosphate buffer (pH 6.5). A 50-μl volume of the 5.0 m*M* 3-HAA solution was applied to the HPLC–ED–UV system and a 200-μl volume of the 3-HAA solution was applied to the HPLC–ED–UV–MS system, immediately after the 3-HAA was dissolved.

2.6. Auto-oxidation of 3-HAA and oxidations of 3-HAA by horseradish peroxidase, by potassium ferricyanide, and by superoxide dismutase

A reaction mixture of auto-oxidation of 3-HAA contained 5 m*M* 3-HAA and 50 m*M* sodium phosphate buffer (pH 6.5). The auto-oxidation of 3-HAA was performed keeping the 3-HAA solution under air in the dark at 25°C for 21 h. A 50-μl volume of the reaction mixture was applied to the HPLC–UV system.

A reaction mixture of 3-HAA with horseradish peroxidase and hydrogen peroxide contained 4.9 m*M* 3-HAA, 1.0 m*M* hydrogen peroxide, 9.3 U/ml horseradish peroxidase and 50 m*M* sodium phosphate buffer (pH 6.5). The reactions were initiated by adding horseradish peroxidase and were carried out for 1 min at 25°C. A 50-μl volume of the reaction mixture of 3-HAA with the horseradish peroxidase and hydrogen peroxide was applied to the HPLC–UV system.

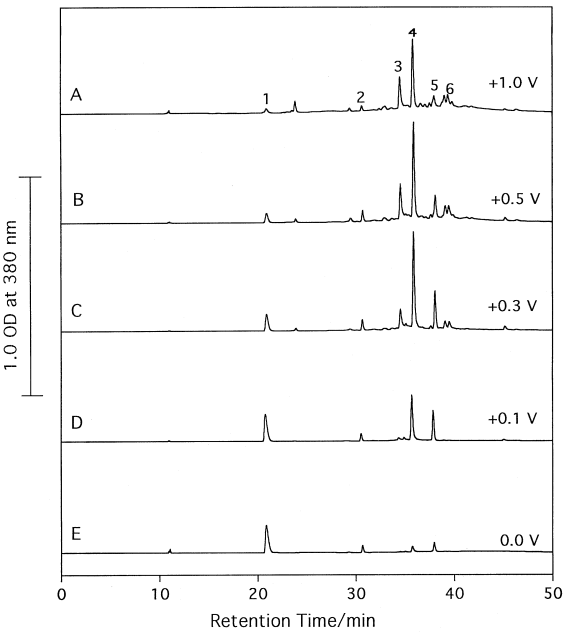

Fig. 1. The UV traces (380 nm) of the HPLC–ED–UV analyses of 3-HAA using the various applied potentials. The HPLC–ED–UV conditions were as described in Experimental. (A) +1.0 V, (B) +0.5 V, (C) +0.3 V, (D) +0.1 V, (E) 0.0 V.

A reaction mixture of 3-HAA with potassium ferricyanide contained 5 m*M* 3-HAA, 18 m*M* of potassium ferricyanide and 50 m*M* sodium phosphate buffer (pH 6.5). The reaction was initiated by adding potassium ferricyanide. The reaction was performed for 1 min at 25°C. A 50-μl volume of the reaction mixture of 3-HAA with potassium ferricyanide was applied to the HPLC–UV system.

A starting reaction mixture of 3-HAA with SOD contained, in a total volume of 730 μl, 4.8 m*M* 3-HAA, 790 U/ml catalase, 960 U/ml SOD and 50 m*M* sodium phosphate buffer (pH 6.5). A 10-μl volume of 58 000 U/ml catalase solution was added into the reaction mixture every hour. The catalase solution was dissolved in 50 m*M* sodium phosphate buffer (pH 6.5). The reaction was performed at 25°C. A 50-μl volume of the reaction mixture of 3-HAA with SOD was applied to the HPLC–UV system every hour. The peak heights, which were observed on the UV trace of 380 nm, were corrected for the concentration change due to the addition of the catalase solution.

3. Results

3.1. HPLC–ED–UV analyses of 3-HAA

3-HAA was analyzed using HPLC–ED–UV (Fig. 1). The analyses were performed using the guard cell of the electrochemical detector with the various

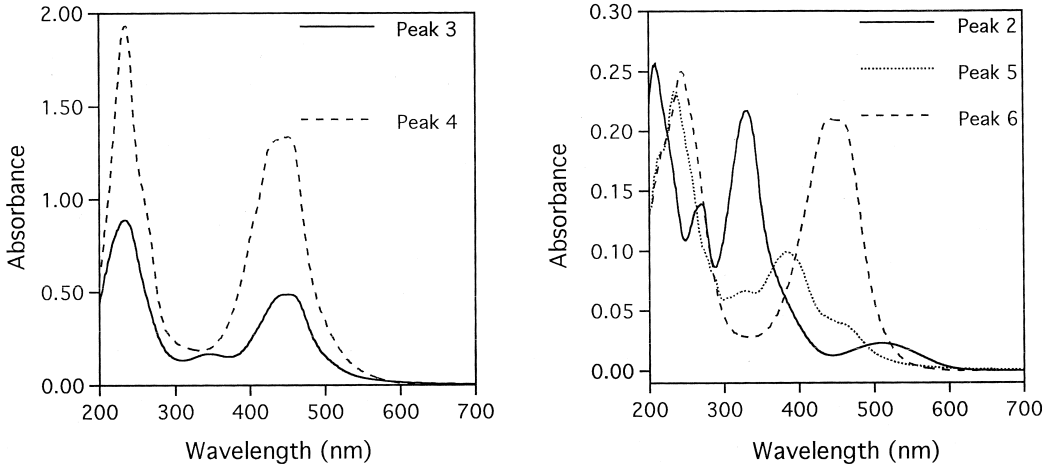

Fig. 2. UV–visible spectra of peaks 2, 3, 4, 5 and 6. UV–visible spectra of peaks 3, 5 and 6 were obtained using HPLC–ED–UV analysis of 3-HAA at +0.5 V of the applied potential. UV–visible spectra of peaks 2 and 4 were measured on the HPLC–UV analysis of the reaction mixture of auto-oxidation of 3-HAA.

applied potentials (0.0 V to +1.0 V). A peak (peak 1) with a retention time of 20.9 (±0.1) min was detected on the UV trace at 380 nm (Fig. 1A–E). Peak 1 is 3-HAA. The peak height decreased with increase of the applied potential, indicating that 3-HAA was oxidized by the guard cell of the electrochemical detector during the HPLC–ED–UV analysis. On the other hand, five prominent peaks (peaks 2–6) were detected on the UV trace at 380 nm at +1.0 V of the applied potential (Fig. 1A). These compounds are presumptively oxidation products from 3-HAA. Their peak heights changed depending upon the applied potentials. The retention times of peaks 2, 3, 4, 5 and 6 are 30.6 (±0.1), 34.5 (±0.1), 35.8 (±0.1), 38.0 (±0.1) and 39.4 (±0.1) min, respectively.

3.2. UV–visible spectra of peaks 2, 3, 4, 5 and 6

UV–visible spectra of peaks 2, 3, 4, 5 and 6 were obtained using diode array detection (Fig. 2). These peaks showed the following λ_{max} values: peak 2, 209 nm, 270 nm, 331 nm and 511 nm; peak 3, 234 nm and 452 nm; peak 4, 234 nm and 452 nm; peak 5, 236 nm, 330 nm and 381 nm; peak 6, 244 nm and 457 nm. Peaks 3, 4 and 6 showed quite similar UV–visible spectra. The λ_{max} values of the peak 2 compound are in fair agreement with the values reported for 6-amino-3-[(2-carboxy-6-hydroxyphenyl)amino]-2,5-dioxo-1,3-cyclohexadiene-1-carboxylic acid [14,15]. On the other hand, the λ_{max} values of the peak 5 compound are also in fair agreement with the values reported for 4,7-diamino-8-methoxy-6H-dibenzo[*a*,*d*]pyran-6-one-3-carboxylic acid ethylester [15].

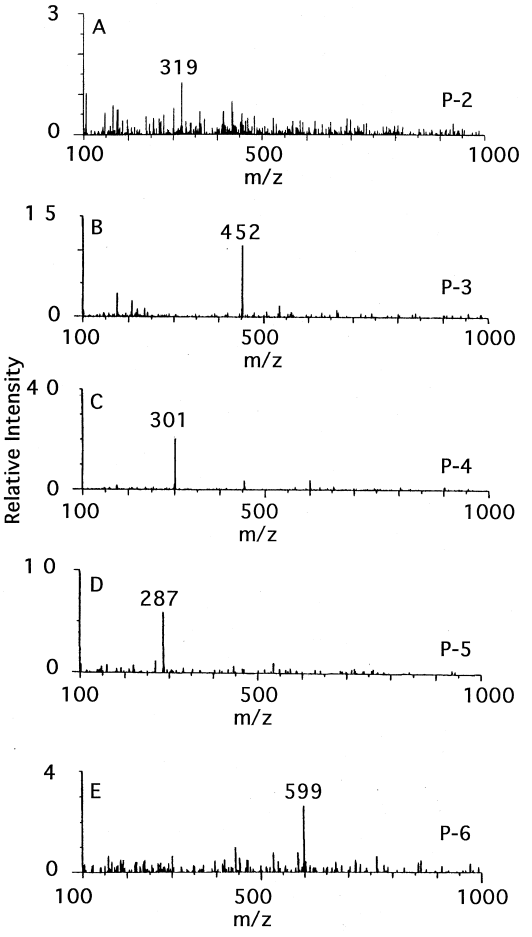

Fig. 3. The HPLC–ED–UV–MS analyses of peaks 2, 3, 4, 5 and 6. The reaction and the HPLC–ED–UV–MS conditions were as described in Experimental. (A) Mass spectrum of peak 2, (B) mass spectrum of peak 3, (C) mass spectrum of peak 4, (D) mass spectrum of peak 5, (E) mass spectrum of peak 6.

3.3. HPLC–ED–UV–MS analyses of 3-HAA

The HPLC–ED–UV–MS analyses of 3-HAA were performed to identify the respective peak compounds. Mass spectra of peaks 2, 3, 4, 5 and 6 are shown in Fig. 3. The mass spectrum of the peak 2 fraction showed a prominent ion of *m*/*z* 319 (Fig. 3A). The ion *m*/*z* 319 corresponds to the $[M+H]^+$ ion of the compound III, 6-amino-3-[(2-carboxy-6-hydroxyphenyl)amino]-2,5-dioxo-1,3-cyclohexadiene-1-carboxylic acid (Fig. 4). Compound III was already identified in the reaction of 3-HAA with molecular oxygen at pH 11.7 [14]. In the HPLC–ED–UV–MS analysis of the peak 3 fraction, an *m*/*z* 452 ion was detected (Fig. 3B). The ion *m*/*z* 452 corresponds to the $[M+H]^+$ ion of the compound IV (Fig. 4). The mass spectrum of the peak 4 fraction showed a peak of *m*/*z* 301 ion (Fig. 3C). The ion *m*/*z* 301 corresponds to the $[M+H]^+$ ion of the compound I, cinnabarinic acid (Fig. 4). The mass spectrum of peak 5 showed an *m*/*z* 287 ion (Fig. 3D). The ion *m*/*z* 287 corresponds to the $[M+H]^+$ ion of the compound II, 4,7-diamino-8-methoxy-6H-dibenzo[*a*,*d*]pyran-6-one-3-carboxylic acid (Fig. 4).

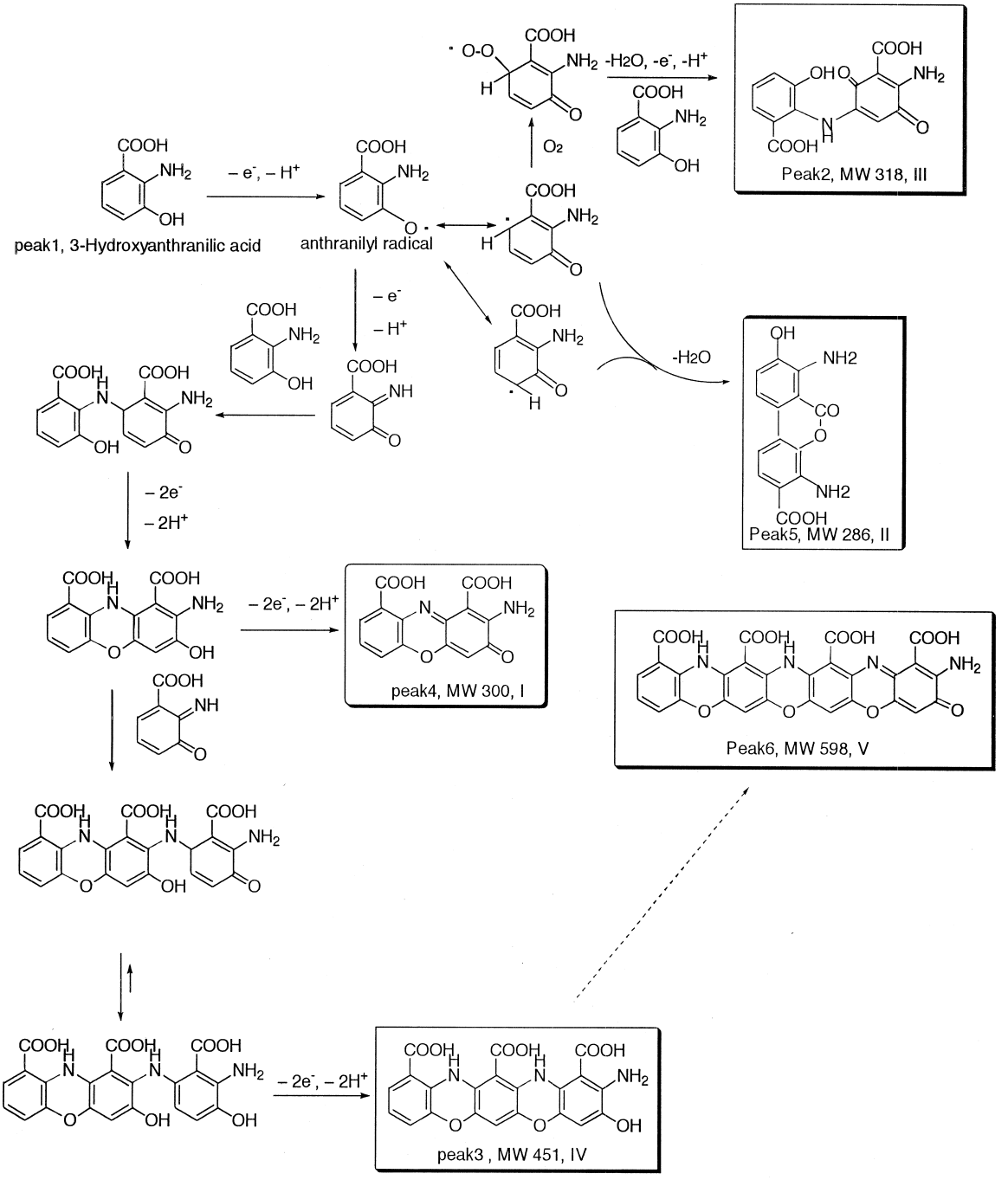

Fig. 4. Possible chemical structures of peak 2, 3, 4, 5 and 6 compounds.

Compound II was already identified in the reaction of 3-HAA with molecular oxygen at pH 7.0 [15]. The mass spectrum of the peak 6 fraction showed a prominent peak of m/z 599 ion (Fig. 3E). The ion m/z 599 corresponds to the $[M+H]^+$ ion of compound V (Fig. 4).

3.4. Auto-oxidation of 3-HAA and oxidations of 3-HAA by horseradish peroxidase, potassium ferricyanide, or superoxide dismutase

The reaction mixture of auto-oxidation of 3-HAA and the reaction mixtures of 3-HAA with H_2O_2 and horseradish peroxidase and of 3-HAA with potassium ferricyanide were analyzed using HPLC–UV (Fig. 5). Similar peaks were detected on the respective HPLC–UV elution profiles of these reaction mixtures. Peak 5 was detected as the highest peak on the HPLC–UV elution profiles of the reaction mixture of auto-oxidation of 3-HAA (Fig. 5B) and the reaction mixture of 3-HAA with H_2O_2 and horseradish peroxidase (Fig. 5C). On the other hand, peak 4 was detected as the highest peak on the HPLC–UV elution profile of the reaction mixture of 3-HAA with potassium ferricyanide (Fig. 5D). This is the case for the reaction mixture of the electrochemical oxidation of 3-HAA at +1.0 V of the applied potential.

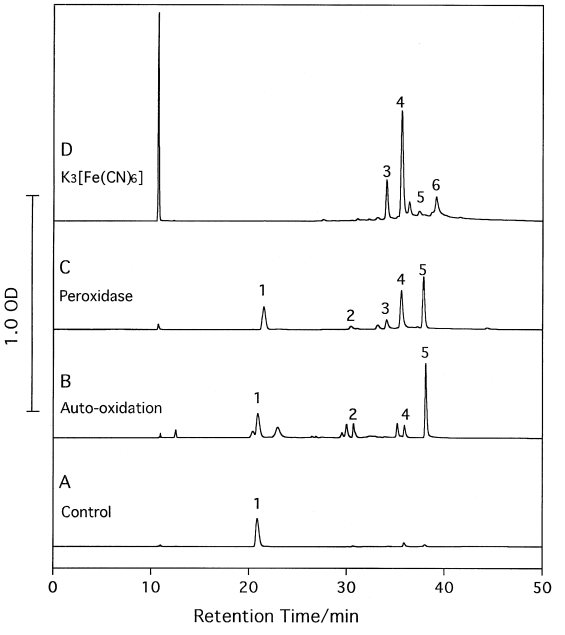

Fig. 5. The HPLC–UV analyses of the reaction mixtures of 3-HAA with H_2O_2 and horseradish peroxidase, of 3-HAA with potassium ferricyanide, and of the auto-oxidation of 3-HAA. Reaction conditions and the HPLC–UV analyses were as described in Experimental. (A) UV trace (380 nm) of the HPLC–UV analysis of the 3-HAA solution, (B) UV trace (380 nm) of the HPLC–UV analysis of the reaction mixture of auto-oxidation of 3-HAA, (C) UV trace (380 nm) of the HPLC–UV analysis of the reaction mixture of 3-HAA with H_2O_2 and horseradish peroxidase, (D) UV trace (380 nm) of the HPLC–UV analysis of the reaction mixture of 3-HAA with potassium ferricyanide.

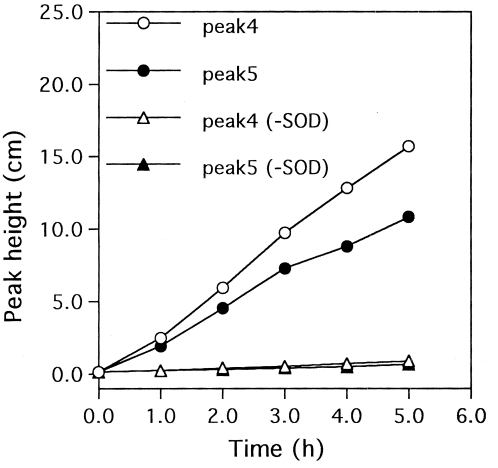

Fig. 6. The effects of SOD on the peak heights of peaks 4 and 5 during auto-oxidation of 3-HAA. Peaks 4 and 5 are peak heights observed on the UV trace (380 nm) of the HPLC–UV of the complete reaction mixture containing 3-HAA, SOD and catalase. Peaks 4 (−SOD) and 5 (−SOD) are peak heights observed on the UV trace (380 nm) of the HPLC–UV of the complete reaction mixture without SOD. Other conditions of the reactions and the HPLC–UV analyses were as described in Experimental.

In order to know the effects of SOD on the oxidation of 3-HAA, time course studies were performed for the reaction mixture containing 3-HAA, SOD and catalase (Fig. 6). The catalase was added every hour to eliminate the H_2O_2 decomposition of cinnabarinic acid [8,18]. The formations of the peak 4 compound and the peak 5 compound were both enhanced by SOD.

4. Discussion

The relative peak heights of peaks 2, 3, 4, 5 and 6 changed depending on the oxidation systems. Com-

pound II (peak 5) is predominant in the auto-oxidation, in the reaction of 3-HAA with horseradish peroxidase and H_2O_2 and in the electrochemical oxidation of 3-HAA at an applied potential of 0.0 V. On the other hand, compounds I, IV and V (peaks 4, 3 and 6) are predominant in the reaction of 3-HAA with $K_3[Fe(CN)_6]$ and in the electrochemical oxidation of 3-HAA at an applied potential of +1.0 V. Above results indicate that the one-electron oxidation product of 3-HAA, anthranilyl radical, forms predominantly during the auto-oxidation of 3-HAA, the reaction of 3-HAA with horseradish peroxidase and H_2O_2, and the electrochemical oxidation at 0.0 V. On the other hand, two-electron oxidation product, quinoneimine, is predominant during the reaction of 3-HAA with $K_3[Fe(CN)_6]$ and electrochemical oxidation at +1.0 V.

Dykens et al. reported that SOD accelerates 3-HAA auto-oxidation by preventing back reaction between superoxide anion and either the anthranilyl radical or the quinoneimine formed during the initial step of the auto-oxidation [18]. It was shown that formations of compound I (peak 4) cinnabarinic acid and compound II (peak 5) 4,7-diamino-8-methoxy-6H-dibenzo[*a*,*d*]pyran-6-one-3-carboxylic acid were both enhanced by SOD in this paper. A possible explanation for the enhancement of the formation of compound I (peak 4) and compound II (peak 5) is the prevention by SOD of the back reaction between superoxide anion and the anthranilyl radical formed during the initial step of auto-oxidation [18]. The other possible explanation for the enhancement of the formation of compound I (peak 4) and compound II (peak 5) is the elimination by SOD of superoxide anions which may decompose cinnabarinic acid and 4,7-diamino-8-methoxy-6H-dibenzo[*a*,*d*]pyran-6-one-3-carboxylic acid. Manthey et al. confirms the decomposition of cinnabarinic acid by superoxide anions [15].

The five 3-HAA-derived oxidation compounds were separated, detected and identified using HPLC–ED–UV and HPLC–ED–UV–MS. These five compounds were identified based on the mass spectra and the UV–visible spectra of the respective peak fractions. Compounds II (peak 5) and III (peak 2) are formed through the one-electron oxidation product of 3-HAA, anthranilyl radical (Fig. 4). On the other hand, conversion of 3-HAA into compound I (peak 4), cinnabarinic acid, is a process of the six-electron oxidation. Compounds IV (peak 3) and V (peak 6) are eight-electron and 12-electron oxidation products, respectively. Fig. 7 shows the applied potential dependence of the peak heights of peaks 3, 4 and 5. Peak 5 reaches a maximum at the lowest applied potential of the three peaks. Peak 3 reaches a maximum at the highest applied potential of the three peaks. On the other hand, peak 2 showed almost the same applied potential dependence as peak 5 (data

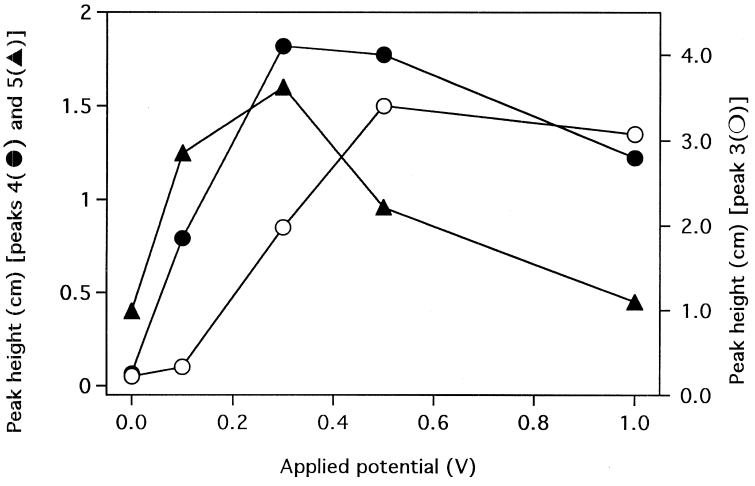

Fig. 7. Applied potential dependence of the peak heights of peaks 3, 4 and 5. The respective peak heights (cm) were observed on the UV trace (380 nm) of the HPLC–ED–UV with various applied potentials.

not shown). Peak 6 resembles peak 3 very closely in the applied potential dependence (data not shown). These applied potential dependence of the peak heights of the respective peaks is consistent with the oxidation processes of the compounds.

In addition to the electrochemical oxidation, various oxidation systems such as auto-oxidation, horseradish peroxidase and $K_3[Fe(CN)_6]$ were employed in this paper. Because any magnitude of the applied potential can be chosen in HPLC–ED–UV–MS or HPLC–ED–UV, the electrochemical oxidation used here is a powerful method in elucidation of redox reactions.

Acknowledgements

This study was partly performed through Special Coordination Funds for Promoting Science and Technology of the Science and Technology Agency of the Japanese Government.

References

[1] S. Christen, E. Peterhans, R. Stocker, Proc. Natl. Acad. Sci. USA 87 (1990) 2506–2510.
[2] S. Christen, S.R. Thomas, B. Garner, R. Stocker, J. Clin. Invest. 93 (1994) 2149–2158.
[3] S.R. Thomas, P.K. Witting, R. Stocker, J. Biol. Chem. 271 (1996) 32714–32721.
[4] M.J. Allen, E. Boyland, C.E. Dukes, E.S. Horning, J.G. Watson, Br. J. Cancer 11 (1957) 212–228.
[5] G.T. Bryan, R.R. Brown, J.M. Price, Cancer Res. 24 (1964) 582–585.
[6] G.T. Bryan, R.R. Brown, J.M. Price, Cancer Res. 24 (1964) 596–602.
[7] W.F. Dunning, M.R. Curtis, M.E. Maun, Cancer Res. 10 (1950) 454–459.
[8] H. Ogawa, Y. Nagamura, I. Ishiguro, Hoppe-Seyler's Z. Physiol. Chem. 364 (1983) 1507–1518.
[9] H. Iwahashi, T. Ishii, R. Sugata, R. Kido, Biochem. J. 251 (1988) 893–899.
[10] W. Prinz, N. Savage, Hoppe-Seyler's Z. Physiol. Chem. 358 (1977) 1161–1163.
[11] S. Christen, P.T. Southwell-Keely, R. Stocker, Biochemistry 31 (1992) 8090–8097.
[12] O. Toussaint, K. Lerch, Biochemistry 26 (1987) 8567–8571.
[13] C. Eggert, U. Temp, J.F.D. Dean, K.E.L. Eriksson, FEBS Lett. 376 (1995) 202–206.
[14] M.K. Manthey, S.G. Pyne, R.J.W. Truscott, J. Org. Chem. 53 (1988) 1486–1488.
[15] M.K. Manthey, S.G. Pyne, R.J.W. Truscott, Biochim. Biophys. Acta 1034 (1990) 207–212.
[16] H. Iwahashi, T. Ishii, J. Chromatogr. A 773 (1997) 23–31.
[17] H. Iwahashi, J. Chromatogr. A 753 (1996) 235–242.
[18] J.A. Dykens, S.G. Sullivan, A. Stern, Biochem. Pharmacol. 36 (1987) 211–217.